Proceedings of the Twenty-second (2012) International Offshore and Polar Engineering Conference **www.isope.org**
Rhodes, Greece, June 17–22, 2012

ISBN 978-1-880653-94–4 (Set); ISSN 1098-6189 (Set)

Vortex Shedding and Vortex-Induced Vibration of Piggyback Pipelines in Steady Currents

Zhipeng Zang, Fuping Gao, Jinsheng Cui
Institute of Mechanics, Chinese Academy of Sciences
Beijing, China

ABSTRACT

The vortex shedding characteristics for submarine pipelines in a sub-critical regime are quantitatively investigated. The swirling strength analysis is conducted on the wake flows around the pipelines. For a single wall-free pipeline, the peak value of the time-averaged nondimensional swirling strength (WD^2/U^2) is almost constant with Reynolds number ($Re = 1.0\times10^4 \sim 4.0\times10^4$). For a pipeline close to the bottom, the peak value of WD^2/U^2 decreases with the decrease of the gap ratio (e/D) when $e/D < 0.3$, owing to the suppression of vortex shedding. For piggyback pipelines near the bottom, the vortex shedding characteristics are dependent on both the gap ratio (e/D) and the spacing ratio (G/D). Four different wake patterns are found in swirling strength fields around the piggyback pipelines. The vortex-induced vibrations of the piggyback pipelines are further conducted and the relationship between the magnitude of swirling strength and the amplitude of vibration is established. It can be concluded that the nondimensional swirling strength is an important parameter in quantifying the vortex shedding and the suppression of vortex shedding.

KEY WORDS: Piggyback pipelines; PIV; swirling strength; vortex shedding; vortex-induced vibration.

INTRODUCTION

Free spans often occur below the submarine pipelines due to the long-term actions of waves and currents or the unevenness of the seabed. Vortex shedding is formed and exerts a periodic transverse force on the spanning pipeline, leading to the vortex-induced vibration (VIV) of the structure. Therefore, the investigation on the mechanism and the suppression of vortex shedding from submarine pipelines has great significance on the design and operation of pipeline engineering.

Sometimes the offshore pipelines of different diameters are laid on the seabed as a bundle for technical and economic reasons. The piggyback pipelines, which consist of a main (large) pipe and a piggyback (small), are the most popular configuration of the pipeline bundles. The proximity of the secondary pipe and the near-wall effect of the seabed influence the flow fields around the pipeline and may suppress the vortex shedding from it in some cases. This would be beneficial to the stability of pipelines.

The conventional submarine pipeline is usually simplified as a circular cylinder near a plane wall. The hydrodynamic forces and the wake flow around the cylinder were mainly studied. Bearman and Zdravkovich (1978), Taniguchi and Miyakoshi (1990), et al, conducted experiments to study the hydrodynamic forces and flow patterns around a circular cylinder near a plane wall. It had been found that regular vortex shedding from a cylinder near a plane wall was suppressed when the gap is less than a certain value. The nodimensional vortex shedding frequency, the Strouhal number (St), is also determined from the experiments. The Particle Image Velocimetry (PIV) was applied by Price et al (2002), Wang and Tan (2008) and Lin et al (2009) to study the flow around a circular cylinder near to a plane wall at different Reynolds number. Not only the flow pattern but also the quantitative information of the vortex shedding from the cylinder was acquired by this whole-field measurement. The characteristics of the vortex shedding from the cylinder and the ensemble-averaged flow fields were found to be strongly dependent on the gap ratio.

The flow around piggyback pipelines is much more complicated than that around a single pipe due to the presence of the piggyback. Chung and Conti (1994) experimentally studied the vortex suppression for a deep-ocean pipe with cables. The results shown that the drag and lift forces were increased significantly when cables are parallel to the pipe. For the pipe straked with helical cable and with a perforated shroud, the vortex shedding from the pipe can be effectively suppressed. Li and Zhang (1994) measured the hydrodynamic forces on piggyback pipelines under combined waves and currents. The relationship between the drag and inertial force coefficients and KC number was drawn from experiments. Kalahatgi and Sayer (1997) found that the existence of the small pipe may increase the drag force of piggyback pipelines by 50%-100% compared with the value for a single pipeline for Reynolds number ranging from 9×10^4 to 3×10^5.

Kamarudin et al (2006) calculated the hydrodynamic forces on piggyback pipelines mounted on a seabed with different position angle. The main cylinder in $\theta=\pi/2$ configuration will experience the highest mean drag, while the maximum lift on the main cylinder occurs with $\theta=\pi/4$ arrangement. Zhao et al (2007) numerically simulated piggyback pipelines near a plane seabed in the steady current. The effects of the spacing (G) between two pipes and the gap (e) between the main pipe and the plane wall on the hydrodynamic characteristics of piggyback pipelines were investigated.

From the above review of the studies on piggyback pipelines, it can be seen that most of studies on this topic are mainly on the hydrodynamic characteristics of the structure. The wake flow pattern and vortex shedding characteristics of piggyback pipelines, which determines the hydrodynamic performance of the structure, has not been comprehensively studied. Till now, there still is a vacancy on the quantitative measurement of the wake flow around the piggyback pipelines and also remain many uncertainties on the vortex shedding from piggyback pipelines.

In general, the experimental studies on the flow around cylinders rely mainly on the flow visualization (hot-film, hydrogen bubble, smoke-line, dye injection, etc.) and single-point measurement (hot-wire, LDV, etc). Although the wake flow pattern and the process of vortex shedding can be captured by a flow visualization method, the quantitative information of the vortex shedding, such as velocity vector, vorticity, swirling strength, Reynolds stress, etc, can not be well obtained. The PIV is used extensively in recent years as a robust flow measurement technique. It can capture the whole–field features, not only observing the wake flow pattern, but also giving the quantitative information of the flow.

So in this paper, a quantitative investigation on the vortex shedding from both single pipeline and piggyback pipelines is conducted with the PIV measurement based on the swirling strength analysis. Then, the vortex-induced vibrations of piggyback pipelines are simulated to study the relationship between the magnitude of swirling strength and the amplitude of vibrations.

EXPERIMENTAL SETUP AND METHODS

The flow measurement was carried out in the wave/current flume at Institute of Mechanics, Chinese Academy of Sciences. The flume is 52.0 m in length, 1.0 m in width and 1.5m in depth. The water depth for experiments is kept at 0.5 m. The ground of the test section in the flume is specially designed with a 1.0 × 1.0 m transparent glass installed at 16.0 m downstream of the flow inlet. Through the transparent glass ground, the pulsed laser sheet can illuminate the whole flow area from the bottom side of the flume. This can well capture the gap flow between the pipe and the plane boundary and also reduce the reflection of the laser by the water surface. The model of main pipe is made of a Plexiglas tube with an outer diameter of D = 80 mm. The piggyback is made of Plexiglas rod with diameter of d = 20 mm. The surface of the model is painted with black color to reduce the reflection of light. The experimental setup is shown in Fig. 1. The length of the pipeline model is 980 mm, which results an aspect ratio of the cylinder span to the diameter of the main pipe (L/D) of >12. This aspect ratio of the experimental model is considered large enough to ensure a 2-D flow in the central region of the near wake, avoiding the boundary effect of the side wall.

A Lavision PIV system was used in the measurements. The double-cavity Nd: YAG laser (power of 135 mJ per pulse, duration of 5 ns) by Litron Lasers was used to illuminate the flow field. The tracer particle with a mean diameter of 55μm and specific density of 1.02 were seeded in the flow. After consecutive exposures, the tracer particle images were recorded on the 12-bit Flow Intense CCD camera, which has a resolution of 1376 × 1040 pixels. The images of the flow field were processed with the DaVis 7.0 software. By comparing each pair of the single-exposed images, the particle displacement was calculated in the cross-correlation mode with the standard cyclic FFT-based algorithm. The multi-pass resolution with the decreasing window size from 64 × 64 pixels, then steps down to the window size of 32 × 32 pixels with an overlapping of 50% was applied. This interrogation and evaluation procedure yielded approximately 5600 velocity vectors (u, v) for each image pair. Based on a compromise between the requirements of recording a large field of view and resolving detailed flow structures, the PIV viewing area for most cases was chosen at 320 × 240 mm (i.e. 4.0 × 3.0 D) in the x-y plane, therefore the spatial resolution is about 3.6 × 3.6 mm (i.e. 0.045 × 0.045 D). For each testing case, a total of 300 samples were acquired at the frequency of 5.03Hz (i.e. ≈ 59.6 s recordings), with the time delay between the double pulses at 500 ns. Following the procedure in Scarano and Riethmuller (1999) for the accuracy analysis due to the limitation of the number of PIV samples, the standard deviation of velocity components u and v in the present experiment was estimated to be 5%.

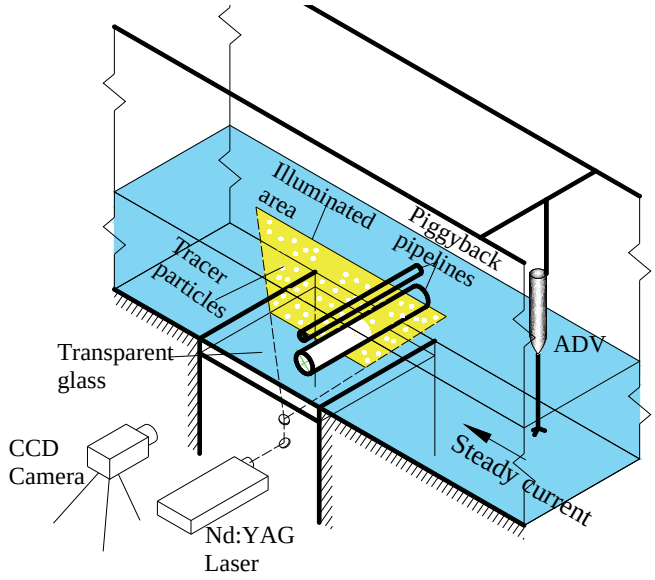

Fig. 1. Experimental setup of PIV measurement

In the past decades, various vortex identification methods have been proposed to interpret the vortical structures in instantaneous velocity fields. But each criterion may have its own constrains and fail in certain situations. For example, the vorticity field may fail in identifying vortices due to its inability to discriminate between shearing and swirling motions. However, the wake flow field around a cylinder near the plane wall is full of swirling motions (vortex shedding from the cylinder) and shearing motions (two shear layers from the top and bottom sides of the cylinder, and the wall boundary layer). A strong shearing flow, like the wall boundary layer can bring high vorticity but it is not a real vortex. So in this study, a generally applicable definition – swirling strength (λ_2 criterion) proposed by Jeong and Hussain (1995), is used to interpret the vortex shedding from structures. This definition is deduced from the discriminant for complex eigenvalues (λ_2), and has been found to represent the topology and geometry of vortex cores correctly for a large variety of flows. For 2-D velocity vectors, it can be expressed as

$$W = \left(\frac{\partial u}{\partial x} + \frac{\partial v}{\partial y}\right)^2 - 4\left(\frac{\partial u}{\partial x}\frac{\partial v}{\partial y} - \frac{\partial u}{\partial y}\frac{\partial v}{\partial x}\right) \quad (1)$$

where, (u, v) represent the horizontal and vertical velocity components. The unit of swirling strength is s^{-2}. In this study, the swirling strength is normalized with the flow velocity U and the diameter of pipe D, expressed as WD^2/U^2. Discussions of this nondimensional swirling strength will be detailed in following section.

For the laminar boundary layer on a plate with a zero incidence, the boundary layer thickness can be estimated at the point where the

velocity reaches 99% of the outer velocity (Schlichting and Gersten, 2000). In this case, the boundary layer thickness is estimated ranging from 0.35 *D* to 0.65 *D*. The flow velocities at 3 m upstream of the model and that above the model are measured with Acoustic Doppler Velocimetry (ADV) and the blockage of the model is estimated at 9%.

FLOW AROUND A SINGLE CIRCULAR CYLINDER

The wake flows around a single pipe are measured and analyzed to validate the accuracy of PIV measurement and the effectiveness of the swirling strength method.

The flow field around a pipe mounted on the bottom was measured at $Re = 1.5\times10^4$. The PIV viewing area is set at a large window of 600 × 450 mm (i.e. 7.5 × 5.6 *D*) to capture the whole wake region. The time-averaged velocity field around the pipe was calculated over the recording period. As shown in Fig. 2(a), a large recirculation zone downstream the pipe is found extending from the upper side of the pipe, up to the flow reattaching to the bottom wall. The length of the primary recirculation zone is estimated about 5.0 *D*, which is in the proper range of the published results. Then the camera was zoomed into a smaller viewing area of 240 × 180 mm (i.e. 3.0 × 2.3 *D*) to capture the flow field in the approximate of pipe. Another small vortex is found at the downstream corner between the pipe and the bottom (in Fig. 2(b)). These vortices are the typical flow characteristics for a pipe mounted on the bottom. It can be seen that present PIV measurement can well capture the flow details around a pipeline.

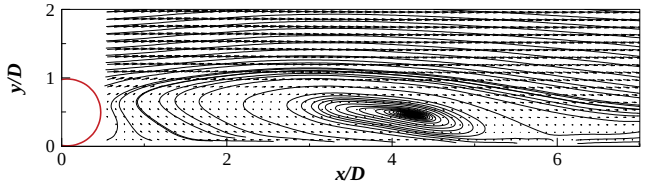

(a) Large recirculation zone

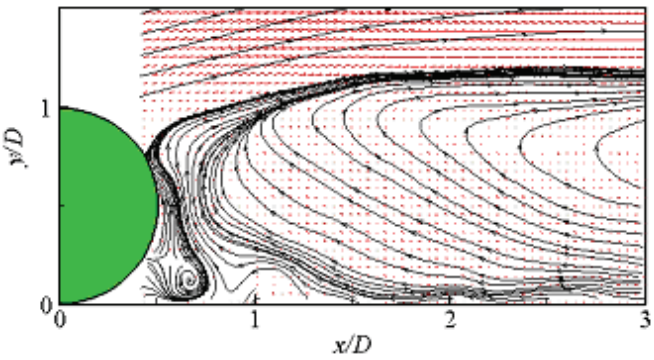

(b) Small vortex at the corner

Fig. 2 Streamlines around a pipe mounted on the bottom, $Re = 1.5\times10^4$

Then, the vortex shedding from a pipe free from the bottom was studied. The time histories of the swirling strength at two fixed points near the top and bottom in the wake region were extracted and analyzed with a FFT method. The energy spectra of the swirling strength are plotted in Fig. 3. The horizontal axis is in the nondimensional vortex shedding frequency, *St*. It can be seen that the dominant frequency of the energy spectra is at about 0.20. Then, the Strouhal number with *Re* ranging from 1.0×10^4 ~ 4.0×10^4 was shown in Fig. 4. It can be seen that *St* is remarkably constant at about 0.2 in this *Re* range, which is very close to the averaged value of *St* reported by many researchers.

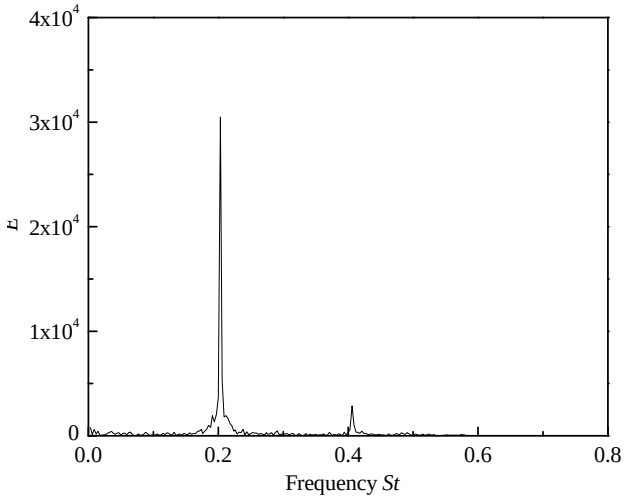

Fig. 3 Energy spectra of *W* near top of cylinder in wake region, $Re = 1.5\times10^4$

For a fluctuated flow field, the time-averaged analysis is a good way to study the basic flow characteristics. So the time-averaged swirling strength fields around the pipe were calculated. Fig. 5(a) is a typical contour plot of WD^2/U^2 around a wall-free pipe at $Re = 1.5\times10^4$. It can be seen that the time-averaged swirling strength field is perfectly symmetric about the centerline of the cylinder. Fig. 5(b) is the counterpart of the streamlines of the flow field. Then, the maximum values of WD^2/U^2 around the pipe under different velocities are calculated and plotted against *Re* in Fig. 6. It can be seen that the peak value of time-averaged WD^2/U^2 doesn't vary much with *Re*. This phenomenon is much similar to that of the vortex shedding frequency varying with *Re* in subcritical regime. For a long time, the frequency of vortex shedding for a cylinder can be quantified with the Strouhal number *St*. Here, it is expected that the normalized swirling strength WD^2/U^2 can represent the strength of vortex shedding quantitatively.

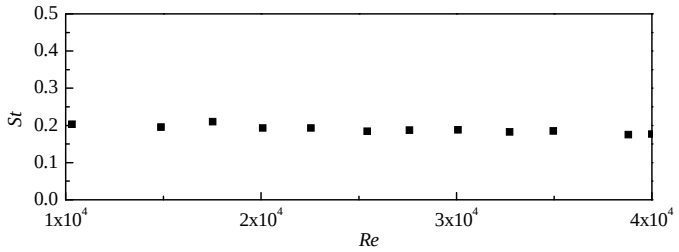

Fig. 4 Strouhal number *St* obtained by FFT analysis of *W* .Vs. *Re*

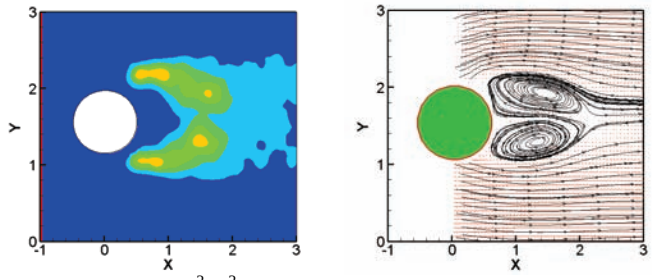

(a) WD^2/U^2 (b) Streamlines

Fig. 5 Time-averaged field around a wall-free pipe, $Re = 1.5\times10^4$

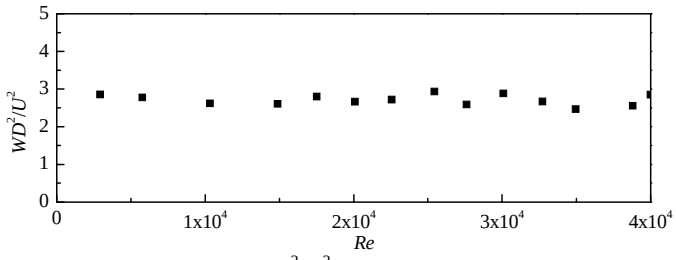

Fig. 6 Maximum value of WD^2/U^2 around a single cylinder .Vs. Re

A study on the vortex shedding characteristics of a single pipe closing to the bottom wall was carried out further. In the processed image results, it was found that the periodic vortex shed from the top of the pipe is counter-clockwise; while that shed from the bottom side of the cylinder is in anti-clockwise direction. Fig. 7 shows the contour plots of the time-averaged WD^2/U^2 around a single pipe at different gap ratios. It can be seen that with the decrease of e/D, the swirling strength at both sides of the pipe also decreases. But the value of WD^2/U^2 below the centerline drops more rapidly than that above the centerline. That means the vortex shedding from the bottom side of the cylinder was suppressed more significantly than that from the top side. The variation of the maximum value of WD^2/U^2 in wake region near the top and bottom of the pipe with e/D was plotted in Fig. 8, respectively. When the gap ratio $e/D > 0.5$, the swirling strength in wake region at both sides of the pipe has the same peak value, that means the vortex shed freely from the pipe with no inhibition. When $e/D < 0.3$, the vortex shed from both sides of the pipe is suppressed significantly by the bottom wall. This conclusion coincides well with the results of most of the researchers. The value of WD^2/U^2 at the bottom side is much smaller than that at the top side.

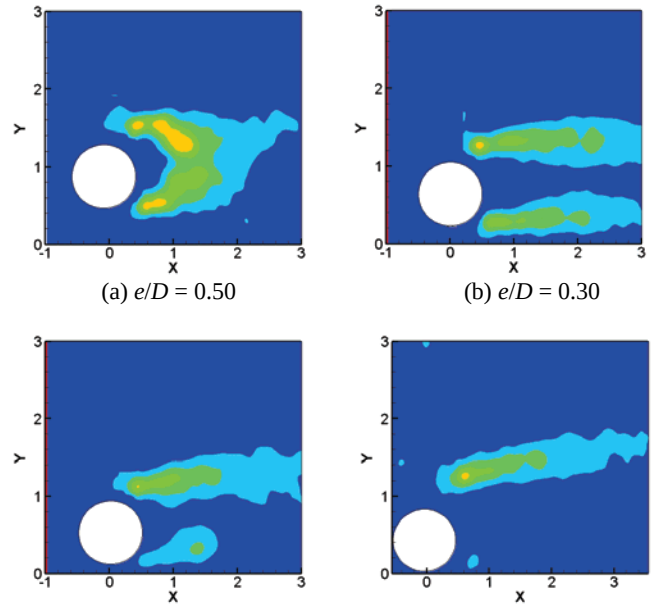

(a) e/D = 0.50 (b) e/D = 0.30

(c) e/D = 0.12 (d) e/D = 0.0

Fig. 7 Averaged WD^2/U^2 field around a single pipe at different gaps, Re = 1.5×10^4

From the above analysis, it is confirmed that the swirling strength can well define the vortex and quantify the intensity of vortex shedding. So in the following section, the swirling strength method will be used to study flow characteristics and the suppression of vortex shedding of piggyback pipelines in steady currents.

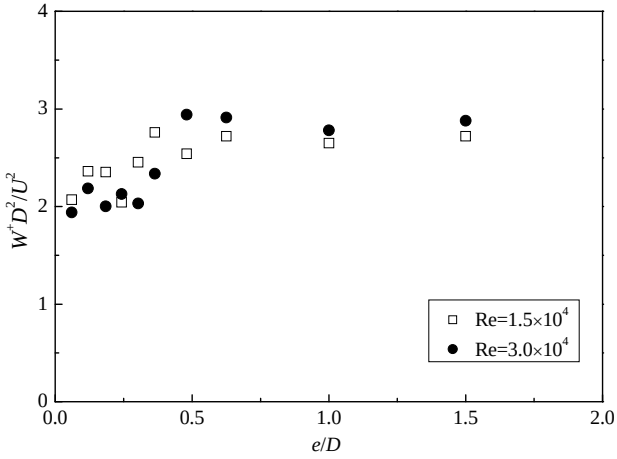

(a) Top side

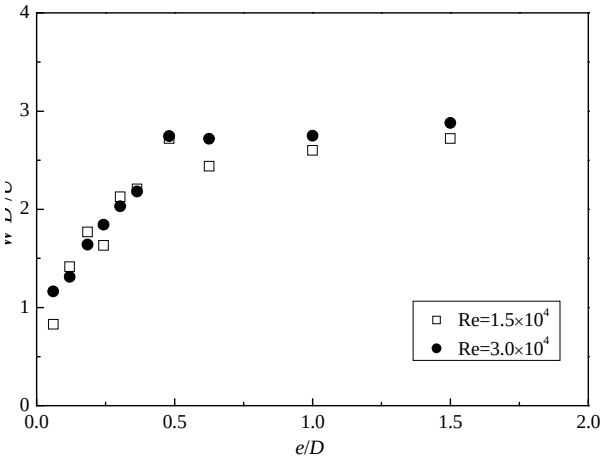

(b) Bottom side

Fig. 8 Maximum value of averaged WD^2/U^2 with e/D

FLOW CHARACTERISTICS OF PIGGYBACK PIPELINES

The wake flows around piggyback pipelines were measured with PIV technique and the averaged fields of WD^2/U^2 over the recording period are analyzed. The gap ratio between the main pipe and the bottom ranges from 0 to 1.0, which means the position of the structure changes from the on-bottom condition to the bottom-free condition. The spacing between the main pipe and the piggyback is 0 ~ 0.5. The measurements were conducted at a flow of Re = 2.2×10^4.

Because the diameter ratio of two pipes is small (d/D = 0.25), the forces on the main pipe dominate the dynamic characteristics of the piggyback pipelines. The intensity of vortex shedding of the main pipe is studied quantitatively. The mean value of time-averaged WD^2/U^2 around the main pipe varying with e/D and G/D are plotted in Fig. 9. The value for a single wall-free pipe (e/D =1.0) is also plotted (solid line) as reference.

Generally, the mean value of WD^2/U^2 decreases with the decrease of e/D. That is to say, the vortex shedding from piggyback pipelines can be effectively suppressed by the bottom wall. For wall-free piggyback pipelines (e/D = 1.0), the mean value of WD^2/U^2 is slightly smaller than that of a single pipe, except for G/D = 0.0 and $G/D > 0.3$. The value of WD^2/U^2 at G/D = 0 and $G/D > 0.3$ is almost equal to that of a single pipe. For G/D = 0, the two pipes behave as a single pipe of an equivalent diameter. A regular vortex shedding is formed behind the

whole body. With the increase of G/D, the two pipes are in a medium distance. Vortex shedding from the main pipe is suppressed to a certain extent by the piggyback under this condition, or the wake flows of the two pipes interfere with each other. The mean value of WD^2/U^2 is not strong as that for a single pipe. But for G/D large enough (> 0.3), the piggyback is far from the main pipe. They behave as two separate single pipes. Therefore, the vortices are shedding freely from two pipes without interference with each other. The mean value of WD^2/U^2 reaches to that for the single pipe.

For other value of e/D, the mean value of WD^2/U^2 has the same trend as that for e/D = 1.0. The mean value of WD^2/U^2 generally decreases with the increase of G/D, then increases and keeps at a constant value thereafter. The mean value of WD^2/U^2 reaches the smallest value at about G/D = 0.12 for $e/D \geq 0.35$, while it reaches the smallest value at about G/D = 0.06 for $e/D \leq 0.20$.

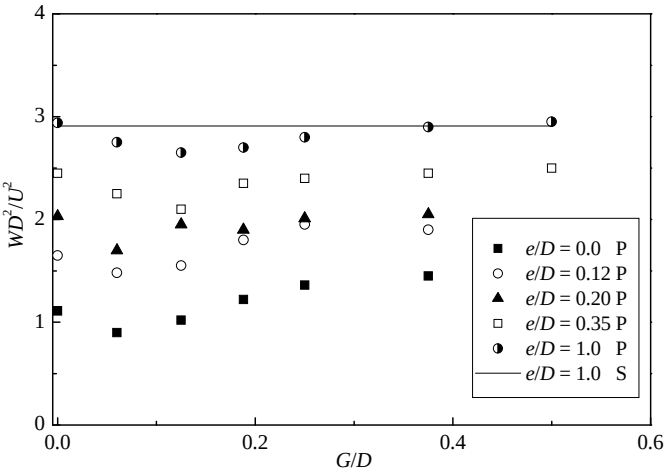

Fig. 9 Maximum value of WD^2/U^2 with different e/D and G/D, Re=2.2×10^4, P −piggyback pipelines, S −Single pipe

Then, the fluctuations of WD^2/U^2 near the top of the main pipe were extracted and analyzed with FFT to study the vortex shedding frequency of the main pipe. Fig. 10 shows the variation of the normalized vortex shedding frequency St with different spacing ratio and gap ratio at 2.2×10^4. It can be seen that the nondimensional vortex shedding frequency of the main pipe generally decreases with the increase of G/D when e/D is set at a constant value. It also can be found that St increases with the increase of e/D. The Strouhal number of the piggyback pipelines in wall-free condition (e/D = 1.0) is almost larger than 0.25. Only when G/D = 0.5 and e/D = 1.0, namely, both the bottom wall and the piggyback are far away from the main pipe, St is about 0.2, which is equal to the vortex shedding frequency for a single pipe. All above can illustrate that both bottom wall and small pipe have influences on the vortex shedding from the main pipe. The vortex shedding from the main pipe can be suppressed to a certain extent by both bottom wall and piggyback.

Owing to the different gap ratio and spacing ratio, the wake flow around the piggyback pipelines shows quite different characteristics. In Fig. 11 (a), for the small gap ratio and spacing ratio, there is no vortex formed at the bottom side of the structure. The two pipes are so close that the piggyback pipelines can be equivalent into a larger pipeline. In this configuration, the periodic vortex shedding was entirely suppressed by the bottom wall. There is only a recirculation region on the top side of the structure in the averaged WD^2/U^2 field.

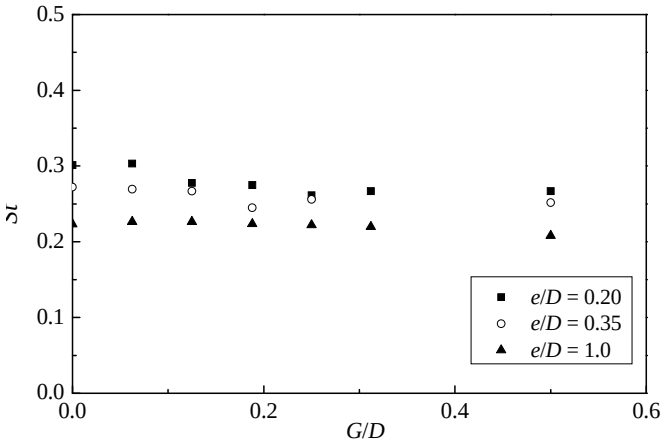

Fig. 10 Strouhal number of piggyback pipelines, Re = 2.2×10^4

In Fig. 11(b), for the large gap ratio and small spacing ratio, the two pipes are close enough to each other and the whole structure is free of the bottom wall. The vortices shed alternatively from both the top and the bottom of the structure as that from a wall-free single pipe. In the swirling strength fields, there two recirculation regions formed at two sides of the structure.

In Fig. 11(c), for the small gap ratio and large spacing ratio, the two pipes are free of each other and the whole structure is close to the bottom wall. The vortex shed from the main pipe is suppressed by the bottom and there is only a recirculation region near the top of the main pipe. As the piggyback is away from the main pipe, the flow characteristic of the piggyback is like that of a single cylinder, the vortex shed periodically from the piggyback. There are two small recirculation regions around the piggyback. There are totally three recirculation regions around the piggyback pipelines.

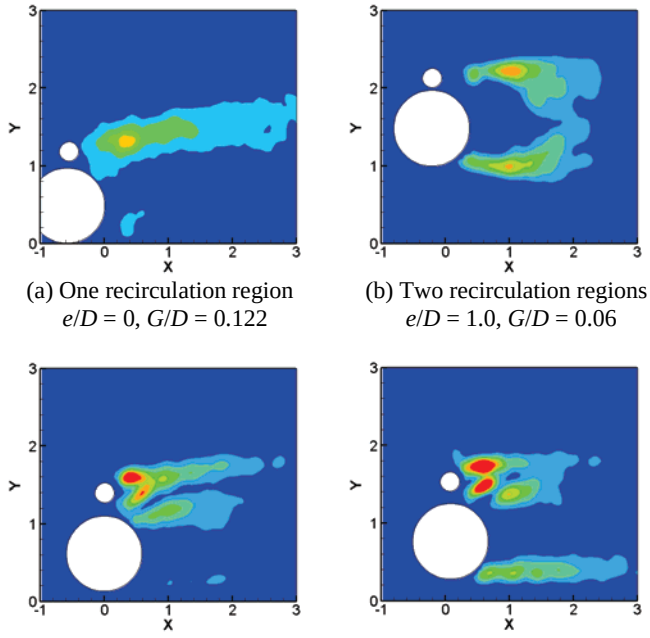

(a) One recirculation region e/D = 0, G/D = 0.122

(b) Two recirculation regions e/D = 1.0, G/D = 0.06

(c) Three recirculation regions e/D = 0.12, G/D = 0.25

(d) Four recirculation regions e/D = 0.3, G/D = 0.25

Fig. 11 Four different wake patterns in the averaged WD^2/U^2 field

In Fig. 11(d), for the large gap ratio and large spacing ratio, the two pipes and the bottom wall are away from each other. The vortices can shed freely from both the main pipe and the piggyback. There are two recirculation regions around each pipe. Therefore, totally four recirculation regions are found around the structure in the averaged swirling strength field.

VORTEX-INDUCED VIBRATION OF PIGGYBACK PIPELINES

As the vortex-induce vibration (VIV) of a pipeline is most direct to the practical engineering, all studies on the vortex shedding characteristics are the basic of the study on VIV and the suppression of it. In this section, the piggyback pipelines model was set flexible to allow the whole structure vibrate freely in the flows to study the dynamic characteristics of the piggyback pipelines. The mass ratio of the whole structure is $m^* = 1.48$; the natural frequency is $f_n = 0.603$Hz; the damping ratio is $\zeta = 0.067$.

The vibrations of the piggyback pipelines with different spacing ratios were measured at three gap ratios $e/D = 0.2$, 0.35, 1.0 at $Re = 2.2\times10^4$. Fig. 12 is the time history of VIV for $e/D = 0.35$, $G/D = 0.5$. It can be seen that the vibration of the piggyback pipelines at this condition is not symmetric about the balance position. The displacement upward (above the equilibrium position) is much larger than that downward (below the equilibrium position). The displacement downward is about 28mm (0.35 D), which is just equal to the initial gap. This is because that the piggyback pipelines are bouncing back when contacting the bottom. Then, it moves upward to the highest point.

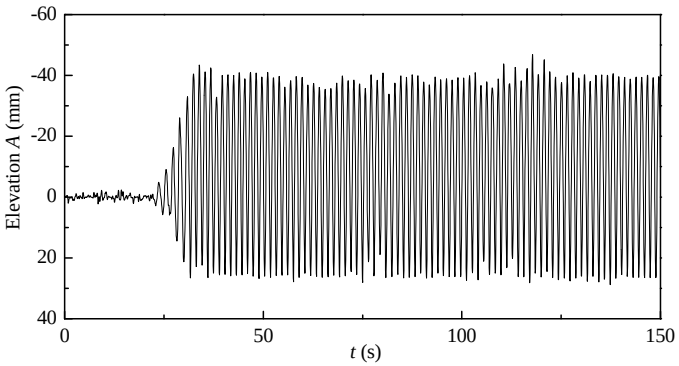

Fig.12 Time history of vibration of piggyback pipelines, e/D=0.35, G/D = 0.5, m^* = 1.48, ζ = 0.067, Re = 2.2×10^4

Fig. 13 compares the maximum (upward) amplitude of the piggyback pipelines during the vibration at different spacing ratio and gap ratio. The amplitude of a single pipe far away from the bottom at the same Reynolds number is also shown in the figure with the averaged value of the amplitude of about 0.8. It can be seen that generally the maximum amplitude of vibration decreases with the decrease of the gap ratio e/D.

For the piggyback pipelines far away from the bottom ($e/D = 1.0$), the amplitude of the vibration decreases with the increase of the spacing ratio when $G/D < 0.2$. When G/D is large than 0.3, the amplitude is almost equal to that of the single pipe. That means that the influence of the piggyback would be ignored when the two pipes are far away from each other. For the gap ratio e/D is 0.35, the value of the amplitude is smaller than that of the single pipe. This is because that the intensity of vortex shedding from the structure was suppressed by the bottom wall. The amplitude of the vibrations decreases with the increase of the spacing ratio when $G/D < 0.2$. When $G/D > 0.3$, A/D doesn't change very much, owing to the weakness of the interaction between the two pipes. For $e/D = 0.2$, the amplitude of vibrations decreases with the increase of the spacing ratio when G/D at a small value ($G/D < 0.06$). Then it increases with the increase of G/D and keeps at a constant value when $G/D > 0.3$. From Fig. 13, it can be seen that the trend of A/D varying with e/D and G/D is much similar to that of WD^2/U^2 shown in Fig. 9. Therefore, it can be concluded that the nondimensional swirling strength WD^2/U^2 is an important parameter in quantifying the strength of vortex shedding from the structure and the suppression of the vortex shedding.

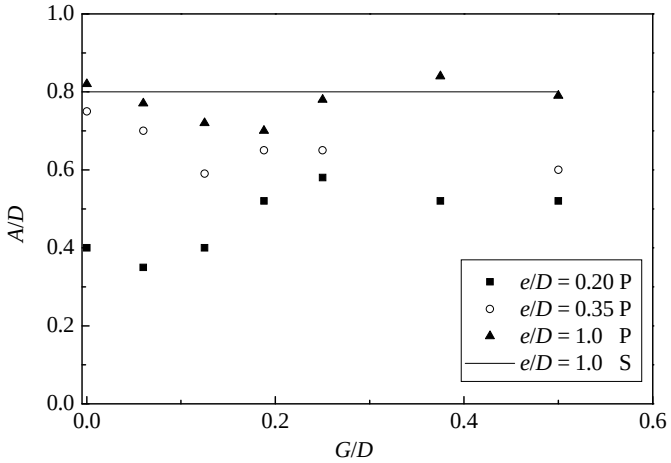

Fig. 13 Maximum amplitudes of vibrations, P −piggyback pipelines, S −single pipe, m^* = 1.48, ζ = 0.067, Re = 2.2×10^4

CONCLUSIONS

In this paper, the wake flow characteristics of submarine pipelines were quantitatively investigated. The swirling strength is analyzed as the key parameter to study the vortex shedding from the pipelines. The swirling strength field around a single pipe is studied first as the benchmark tests to verify the effectiveness of the swirling strength method. The vortex shedding characteristics of the piggyback pipelines are studied based on the swirling strength analysis. Then the vortex-induced vibration of the structure is conducted to study the relationship between the swirling strength and the amplitude of the vibration. The conclusions from this study can be drawn as below:

(1) For a single pipe far away from the bottom, the frequency of the fluctuation of the swirling strength in the near wake is almost constant (at value of about 0.2) with the variation of Reynolds number (1.0×10^4 ~ 4.0×10^4). The maximum value of nondimensional swirling strength WD^2/U^2 is also not dependent much on Reynolds number.

(2) For a single pipe near the bottom, the maximum value of WD^2/U^2 decreases with the decrease of the gap ratio e/D, when $e/D<0.3$, owing to the suppression of vortex shedding by the bottom; when $e/D>0.5$, the suppression of vortex shedding is not significant, the maximum value of WD^2/U^2 is kept constant.

(3) For piggyback pipelines, the maximum value of WD^2/U^2 around the main pipe is dependent on both e/D and G/D. Four different wake patterns of the piggyback pipelines were found in the averaged swirling strength fields.

(4) For the vibrating piggyback pipelines, the amplitude of the vibration is dependent on both e/D and G/D; the trend of A/D varying with e/D and G/D is similar to that of WD^2/U^2 varying with e/D and G/D. That means that WD^2/U^2 is an important parameter in quantifying the vortex shedding and the suppression of vortex shedding.

ACKNOWLEDGEMENTS

This work is financially supported by National Natural Science Foundation of China (Grant No. 51109202).

REFERENCES

Bearman, PW, Zdravkovich, MM (1978). "Flow around a circular cylinder near a plane boundary," *Journal of Fluid Mechanics*, Vol 89, No 1, pp 33–47.

Chung, JS, Conti, RJ (1994). "Flow-Induced Torsional Moment and Vortex Suppression for a Circular Cylinder with Cables," *Proceedings of the Fourth International Offshore and Polar Engineering Conference*, ISOPE, Osaka, Japan, Vol 3, pp 447-459.

Grass, AJ, Raven, PWJ, Stuart, RJ, Bray, JA (1984). "The influence of boundary layer velocity gradients and bed proximity on vortex shedding from free spanning pipelines," *Journal of Energy Resources Technology*, Vol 106, pp 70-78.

Jeong, J, Hussain, F (1995). "On the identification of a vortex," *Journal of Fluid Mechanics*, Vol 285, pp 69-94.

Kalahatgi SG., Sayer PG (1997). "Hydrodynamic forces on piggyback pipeline configurations," *Journal of Waterway, Port, Coastal and Ocean Engineering*, Vol 123, No 1, pp 16-22.

Kamarudin, MH., Thiagarajan, KP, Czajko, A (2006). "Analysis of current-induced forces on offshore pipeline bundles," *Fifth International Conference on Computational Fluid Dynamics in the Process Industries*, Australia, Vol 1, pp 1-6.

Li, Y, Zhang, NC (1994). "The hydrodynamic characteristic of submarine piggyback pipeline in wave-Current coexisting Field," *Proceedings of the Fourth International Offshore and Polar Engineering Conference*, ISOPE, Osaka, Japan, Vol 1, pp 10-15.

Lin, W. J, Lin, C, Hsieh, SC, Dey, S (2009). "Flow Characteristics around a Circular Cylinder Placed Horizontally above a Plane Boundary." *Journal of Engineering Mechanics*, Vol 135, No 7, pp 697-716.

Price, SJ, Sumner, D, Smith, JG, Leong, K, Païdoussis, MP (2002). "Flow visualization around a circular cylinder near to a plane wall," *Journal of Fluids and Structures*, Vol 16, No 2, pp 175-191.

Schlichting, H, Gersten, K (2000). "Boundary-layer theory". Springer-Verlag, Berlin Heidelberg.

Taniguchi, S, Miyakoshi, K (1990). "Fluctuating fluid forces acting on a circular cylinder and interference with a plane wall. Experiments in Fluids", Vol 9, pp 197- 204.

Wang, XK, Tan, SK (2008). "Near-wake flow characteristics of a circular cylinder close to a wall," *Journal of Fluids and Structures*, Vol 24, pp 605-627.

Zhao M, Cheng L, Teng B (2007). "Numerical modeling of flow and hydrodynamic forces around a piggyback pipeline near the seabed.," *Journal of Waterway, Port, Coastal and Ocean Engineering*, Vol 133, No 4, pp 286-295.